

Physical, morphological and mineralogical properties of ceramic brick incorporated with Malaysia's Rice Hush Ash (RHA) agricultural waste

Aneis Maasyirah Hamzah^a, Siti Koriah Zakaria^a, Siti Zuliana Salleh^a, Abdul Hafidz Yusoff^a, Arlina Ali^a,
Mardawani Mohamad^a, Mohamad Najmi Masri^a, Sharizal Ahmad Sobri^a, Mustaffa Ali Azhar Taib^b,
Faisal Budiman^c and Pao Ter Teo^{a,*}

^aAdvanced Materials Research Cluster, Faculty of Bioengineering and Technology, Universiti Malaysia Kelantan, Jeli Campus, 17600 Jeli, Kelantan, Malaysia

^bDivision of Advanced Ceramic Materials Technology, Advanced Technology Training Center (ADTEC) Taiping, 34600 Kamunting, Perak, Malaysia

^cSchool of Electrical Engineering, Telkom University, Bandung 40257, West Jawa, Indonesia

In this work, the effect of various weight percentage of rice husk ash (RHA) in ceramic brick production was investigated in terms of mineralogical, physical, chemical and morphological properties. The evaluation of the use of RHA as a raw material for ceramic products is tested to determine the linear shrinkage, volumetric shrinkage, water absorption, apparent density and bulk density. These physical results suggested that the addition of RHA can improve the physical properties of ceramic brick. Scanning electron microscopy images confirmed the increased of ceramic strength with the addition of RHA and firing temperature. In addition, quantitative and qualitative chemical analysis supported the results obtained. Overall, the results demonstrated the high potential of RHA in green technology for ceramic production.

Keywords: Rice husk ash (RHA) agricultural waste, ceramic brick, green technology, sustainable construction material, RHA-clay brick properties.

Introduction

In Malaysia, the production of paddy is increased with 2.7%, which contributed to 2,639.9 thousand tonnes in 2018 [1]. It can be expected that the by-product waste generated from rice paddy production increase steadily. Rice husk (RH) is a by-product of the industrial processing of rice [2, 3] where approximately 0.23 tons RH is generated from every ton of rice produced [4]. In fact, although RH is categorized as waste or by-product, it contains valuable compositions such as cellulose (38.3%), hemicellulose (31.6%), lignin (11.8%) and silica (18.3%) [5].

In addition, the burning of RH can transform its initial weight around 25% into ash called as rice husk ash (RHA) [2, 6] which contains more than 90% silica [7, 8]. RHA is composed primarily of silica, in amorphous or crystalline form depending on combustion conditions [9]. The crystalline and amorphous forms of silica have different properties, and it is significant to produce ash with correct specifications for specific end-use [10].

Main uses of RHA have been identified which is as an insulator in the steel industry, as a pozzolan in the

cement industry, as a filler in rubber and civil construction works as well as in the advance application such as a ceramic filter for nanofiltration process in the bioreactor [11-15]. In this stance, converting RHA into a new potential application is able to reduce waste disposal impact on the environment [16, 17], which consequently can create environment sustainability with zero secondary wastes.

The highly potential is to use waste in civil construction works because it is well known that ceramic has high tolerance in accepting different materials due to heterogeneous natural ceramic raw materials [18, 19]. Furthermore, in Malaysia, the demand for bricks productions is expected to increase quickly. The unit price index for bricks and wall that are important and prevalent building material keeps increasing according to the Department of Statistics Malaysia, as reported in November 2020 [20]. Hence, the approach to recycle by-product from agriculture waste such as RHA into ceramic productions is expected to provide low-cost brick material with promising required properties.

Other countries, mainly rice-producing nation, have also observed the surge in the utilization of RHA as a raw material in ceramic production. For instance, in Italy, a study by Andreola et al. have found that high silica content in RHA can reduce the plasticity of the ceramic body. Moreover, it shows the positive impact

*Corresponding author:
Tel : +609-9477427
Fax: +609-9477402
E-mail: teopaoter@umk.edu.my

on linear shrinkage and negative impact on water absorption, which is favourable in ceramic production [21]. Moreover, RHA can be used to replace silica gel partially in the production of porous ceramic [22]. On the other hand, in Brazil, Fernandes et al. have conducted a preliminary study on the local RH regarding the suitability as ceramic raw material. It is found that high-silica RHA, which has the potential to be used in the ceramic material, can be produced via thermal treatments [23]. With the recognized potential worldwide, it is worth it to investigate the RHA available in Malaysia.

Therefore, the main aim of this present research is to evaluate the potential of Malaysia's RHA agricultural waste utilization in ceramic bricks production. This preliminary evaluation consisted of the determination of physical and morphological properties of ceramic with various contents of RHA and firing temperature. The investigation on the mineralogical characteristics by X-ray diffraction analysis also presented in this research for more understanding of the phase changes due to the addition of RHA and temperature.

Materials and Method

Materials

The RHA is obtained from Syarikat Beras Bernas Sdn Bhd (BERNAS), Penang, Malaysia as one of the largest rice processing company in Malaysia. The RHA is generated from incineration of rice husk for "local white rice" in Malaysia. The received RHA was burned at temperature 700 °C. In the meantime, China clay was supplied from Kaolin (Malaysia) Sdn. Bhd, Selangor. Then, the ceramic bricks with different contents of RHA are prepared based on body formulation, as shown in Table 1.

Methodology

At first, the RHA-based ceramic bricks production is started with the addition of water into each body formulation, as shown previously in Table 1 in order to form a slurry solution. The mixture was mixed for 30 minutes. Then, the solution was poured into a mould and dried in an oven overnight.

After the drying process, the solid material was ground by using mortar to obtain finely powder form. This followed with placing the powder inside steel die for shaping purpose under the pressing process. During the pressing process, the fine powder is compressed to bind all the powder and form a single compact material

Table 1. Body formulation of raw materials.

Sample	Weight percentage (wt. %)	
	RHA	China Clay
R00	0	100
R20	20	80
R40	40	60

using a hydraulic press of 2000 psi pressure. Two different sizes of the green body were prepared; 1 and 4 cm in diameter.

The last step was thermally heated the green body at different temperatures; 900, 950 and 1,000 °C. The summary of this experimental step is shown in the flowchart as shown in Fig. 1.

Characterizations and testing

The chemical composition of raw material in this research such as clay and RHA was investigated by using Bruker S2 Ranger X-ray Fluorescence spectrometer. Then, the properties of fired RHA-based ceramic bricks were tested. The values of firing shrinkage and volumetric shrinkage were determined by ASTM D427 method. Meanwhile, water absorption, apparent porosity and bulk density were determined according to ISO 10545-3:1995(E).

In addition, X-ray diffraction (XRD) analysis performed by Bruker D2 Phaser X-ray diffractometer and Difffrac. EVA software to analyze the diffractogram patterns also has been employed in the determination of ceramic bricks patterns with different contents of RHA at different heating temperatures. Finally, the microstructure and morphology of the RHA-based ceramic surfaces are investigated by Scanning Electron Microscope (SEM).

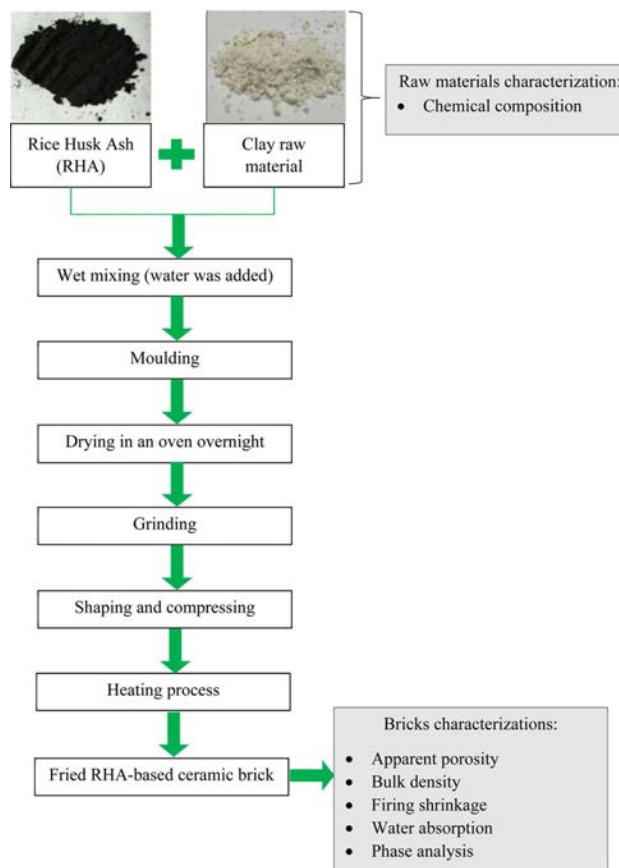


Fig. 1. Flowchart for utilization of RHA in ceramic brick manufacturing.

Results and Discussion

Chemical composition of raw materials

The chemical compositions of RHA and China clay as determined via the XRF analysis are tabulated in Table 2. It can be noticed that the major component of RHA contains silicon oxide (SiO_2), which is about 93.67%. In addition, the value of SiO_2 is higher in RHA than in China clay. This indicates that RHA has a great potential to increase the strength of ceramic [24]. This can be related to the higher fluxing oxides content contributes to the liquid phase formation thorough eutectics that favour the sintering process [25]. Thus, it can be expected that higher oxide, especially SiO_2 content, improves the properties of brick.

Physical properties (Shrinkage, Water Absorption, Apparent Porosity and Bulk Density)

The effects of different RHA contents and firing temperatures on the linear shrinkage (%) of ceramic with different green body sizes; 1 and 4 cm in diameter is shown in Fig. 2(a) and (b), respectively. It is noticeable that the linear shrinkage (%) value is kept increasing with the content of RHA and firing temperature for the sample with 4 cm in diameter (Fig. 2 (b)). Meanwhile, Fig. 2(a) showed a slight difference for the linear shrinkage (%) values with the rising amount of RHA and firing temperature for samples with 1 cm in diameter. As a comparison, the linear shrinkage (%) value is lower for 4 cm diameter samples than 1 cm diameter sample. This observation can be explained by higher thermal exposure in the green body for smaller size samples than in bigger size. This indicates that the size of the green body also influenced the linear shrinkage (%) of ceramic.

Linear shrinkage or expansion behaviour is attributed to the change in the linear dimension of the test samples during heat treatment [3]. Overall, high firing temperature causes high linear shrinkage in all of the samples. Such behaviour could be associated with the densification evolution, which decreases the surface

area of the product, reducing the porosity of the final ceramic and thus increasing its linear shrinkage [25]. In addition, shrinkage also occurs owing to evaporation of the water between clay particles [26], which causes the particles to move closer together [27].

Besides that, the other factor that can be noticed is the increase the linear shrinkage (%) due to the addition of RHA. Opposite observation is reported by Loryuenyong et al. (2009) where they stated that the reduction trend of linear shrinkage with the addition of RHA indicates the effective behaviour of rice husks as a shrinkage barrier [28]. The current result indicates that RHA can promote clay sintering via unstable pore formation, which enhanced the grains rearrangement. These unstable pores collapsed due to densification process that occurred at high temperature. This phenomenon can be expected due to high sintering temperatures. It was reported that shrinkage is influenced by clay sintering and grain reorganization when the temperature is higher than 950°C [29]. It partially melts, resulting to tighten up the interaction between the bonds and also causing the ceramic to have rock-like characteristics [30].

Fig. 3 represents a volumetric shrinkage (%) of ceramics with different amount of weight percentage of RHA which were fired at different temperatures. The addition of RHA also caused the volumetric shrinkage to increase at any firing temperature. As a comparison, the sample with small dimension in Fig. 3(a) showed higher volumetric shrinkage (%) than the bigger sample

Table 2. Chemical composition of raw materials.

Compound	Weight Percentage (wt.%)	
	China clay	Rice Husk Ash
SiO_2	57.63	93.67
Al_2O_3	37.77	1.45
Fe_2O_3	-	0.47
CaO	0.35	1.30
MgO	0.60	0.57
K_2O	1.82	1.80
Na_2O	-	0.54
TiO	0.61	-
ZnO	-	0.1
CuO	-	0.1

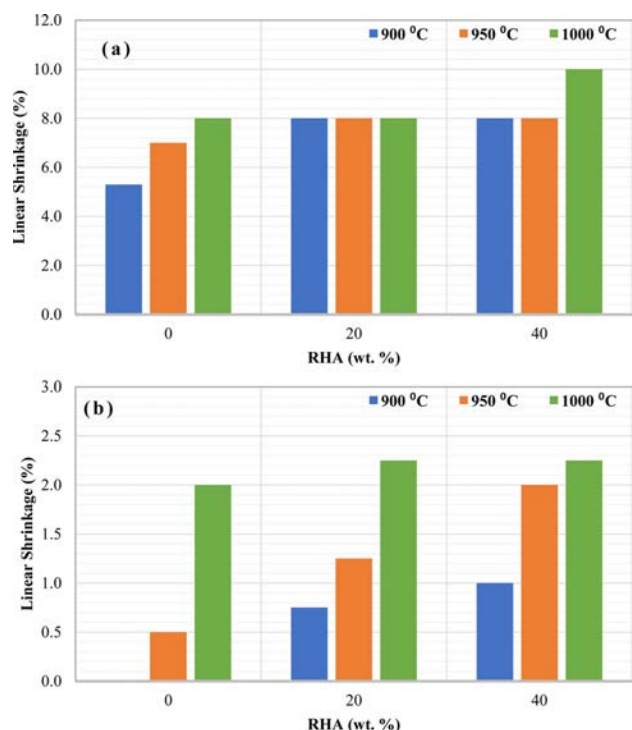


Fig. 2. Linear shrinkage of ceramic with varies amount of RHA and firing temperature for different green body sizes (a) 1, and (b) 4 cm in diameter.

in Fig. 3(b). This again can be explained that small samples are highly exposed to heat which greatly increases the volumetric shrinkage of the sample.

The volumetric shrinkage showed the highest values at the highest temperature with the highest content of RHA. This indicates that the addition of RHA also influences the volumetric shrinkage in RHA-based ceramic brick. This again can be explained due to the combustible RHA at high temperature [24] and the degradation is worsening at higher temperatures.

The effect of varies amount of RHA and firing temperature on water absorption (%) is shown in Fig. 4. The determination of water absorption is a crucial factor which influencing the durability of clay bricks because water can infiltrate bricks and decrease their strength [27]. Lower quantities of water absorbed by ceramics products result in greater durability and resistance [25]. This making RHA as an alternative of raw material for ceramic brick production. In addition, at higher firing temperature, the water absorption is the lowest. At higher temperature, the flowability of SiO_2 is increased and also facilitate gas elimination to promote densification [31]. In addition, high content of RHA indicates a high content of SiO_2 , which consequently responsible for low pore formation in the ceramic bricks.

The abovementioned results showed that the small size of samples (1 cm in diameter) is greatly influenced by heat, and the effect of RHA is neglected. Hence, further discussion of the properties of ceramic with

varies amount of RHA and firing temperature has proceeded with the sample size 4 cm in diameter only.

The other physical properties investigated in this work are shown in Fig. 5(a) and (b) which represent the apparent porosity and bulk density, respectively. It can be distinguished that the apparent porosity decreased with increasing RHA content in the body composition, as shown in Fig. 5(a). Besides that, the increasing firing temperature also decreased the value of apparent porosity. The obtained results are related to the RHA, which contains amorphous active silica. This type of silica is responsible for diffusion reaction with other grains while increasing the sintering temperature above 800°C [3]. This reaction leads to the elimination of pores and thus decreased the apparent porosity. This result also consistent with the results obtained previously

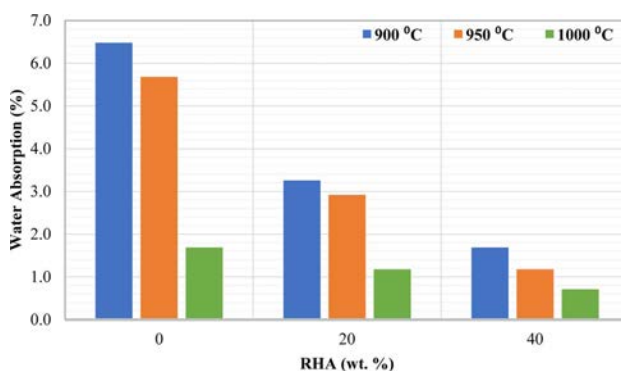


Fig. 4. Water absorption of ceramic with different RHA content and firing temperature.

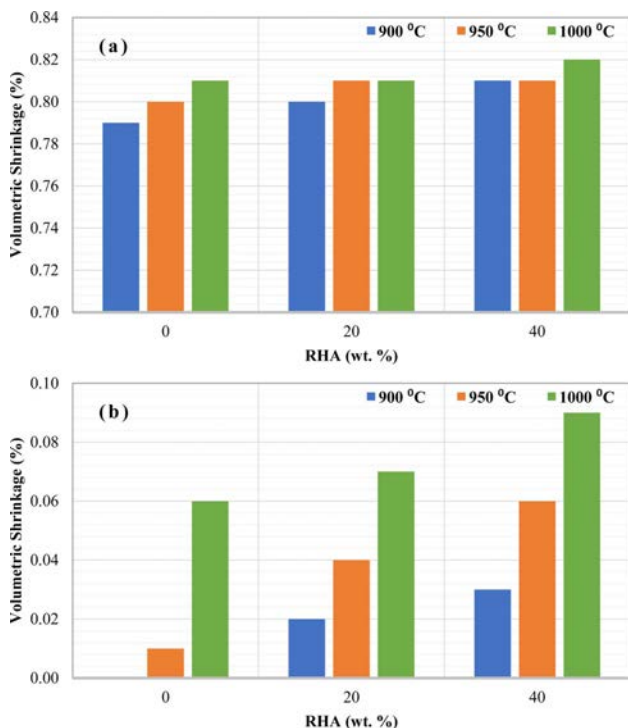


Fig. 3. Volumetric shrinkage of ceramic with varies amount of RHA and firing temperature for different green body sizes (a) 1, and (b) 4 cm in diameter.

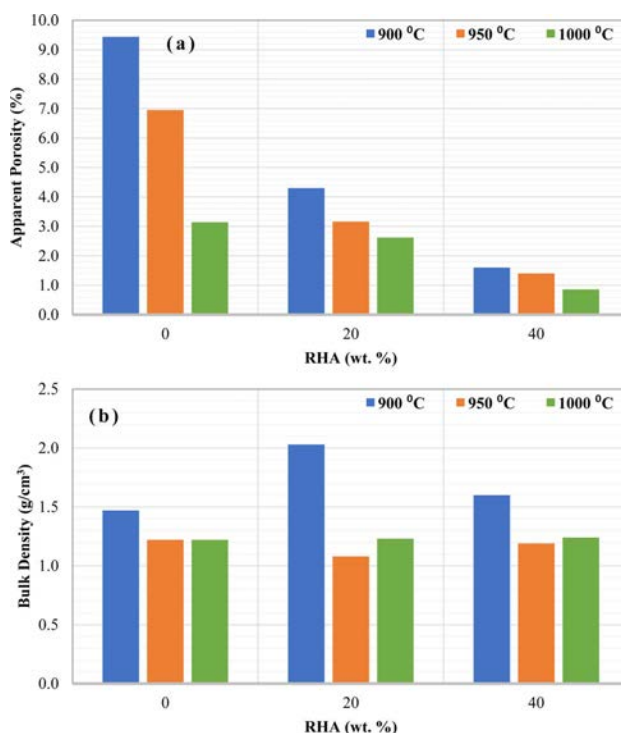


Fig. 5. (a) Apparent porosity and (b) bulk density of ceramic with different RHA contents and firing temperature.

where the addition of RHA increased the linear shrinkage and volumetric shrinkage but decreased the water adsorption.

In general, the apparent porosity is not only directly proportional to the water absorption but also indirectly proportional to the bulk density [27]. Interestingly, it can be noticed in Fig. 5(b) where the bulk density is not affected significantly by the proportion of RHA, especially at high firing temperature. A work reported by Janbuala and Wasanapiampong (2015) observed a decrement of density with the addition of RHA. They stated that the reduction in density is due to the decomposition of RHA at 900 °C and high content of RHA caused more degradation in the sample at the same temperature [32]. Based on this theory, the bulk density of RHA-based ceramics should be lower at higher temperature and content of RHA. The result obtained for 20 and 40 wt.% at a higher temperature (950 °C and 1,000 °C) are fitted with this theory. This indicates that the addition of RHA can produce light-bricks at a higher temperature (≥ 950 °C).

Morphological property

The effect of different RHA content and firing

temperature on the morphological of ceramic is shown in Fig. 6 under the same magnification (2500 \times). It can be pointed out that Fig. 6(a) which represent R40 at 950 °C depicted a rough surface and larger pore as compared to the other SEM images. This image supported previous observation where the porosity of RHA-based ceramic bricks is influenced by the RHA content and firing temperature. For instance, the porosity of RHA-based ceramic brick is the highest at 40 wt.% of RHA which is fired at 900 °C.

The surface of various RHA contents at 1,000 °C as shown in Fig. 6(b-d) displayed rough surface but with less porosity and relatively smoother with an appearance of consolidated microstructure as compared to Fig. 6(a). This indicates that microstructure changed with the addition of RHA content and firing temperature.

The microstructure showed in Fig. 6(b-d) also supports previous results in physical properties of RHA-based ceramic bricks. In general, the decrement of water adsorption and apparent porosity can be explained by the presence of amorphous silica phase which caused partial densification of the ceramic through a viscous flow which fired at high temperature [33]. This explanation can be supported later by XRD analysis

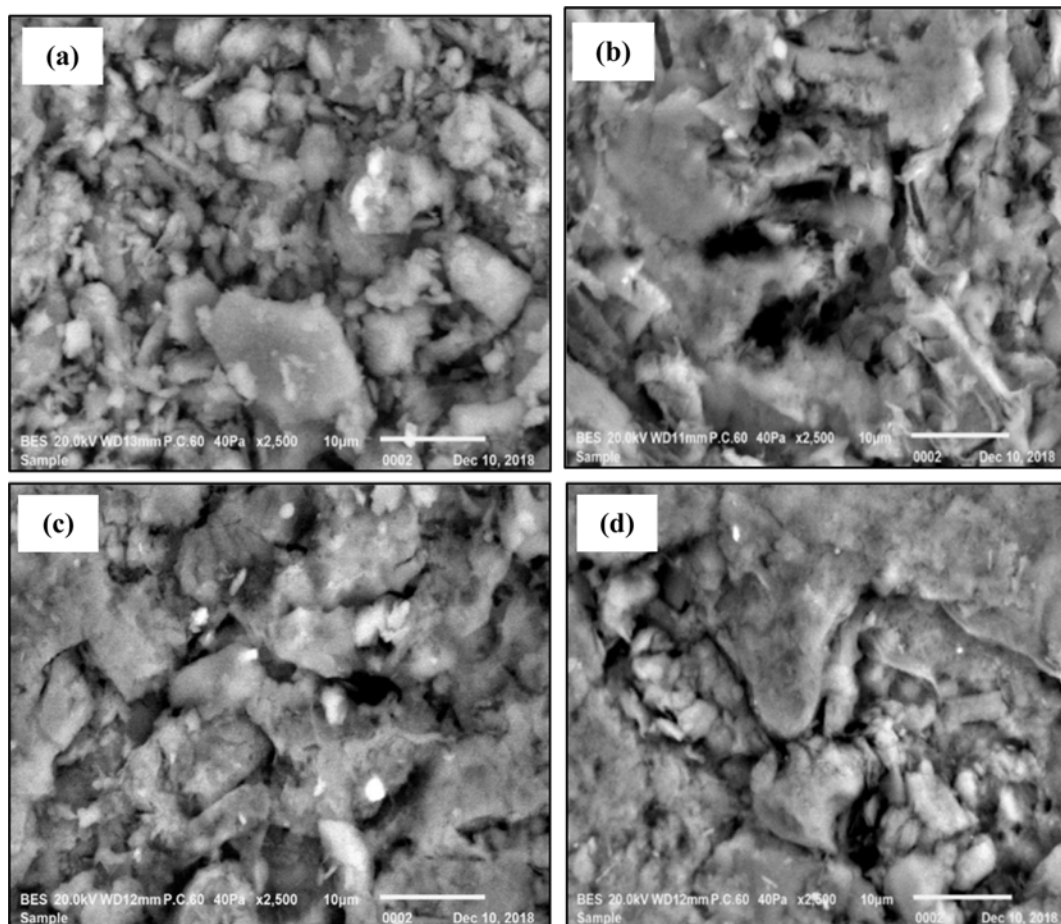


Fig. 6. SEM images of ceramic with different RHA content and firing temperature at 2500 \times magnification; (a) R40 at 950 °C, (b) R00 at 1,000 °C, (c) R20 at 1,000 °C, and (d) R40 at 1,000 °C.

which can detect the presence of amorphous of silica (SiO_2) and other mineralogy compositions. This indicates that the replacement of China clay by RHA caused liquid phase formation increased, resulting in less formation of porosity because the pores are filled during the firing.

Mineralogical property

The phase presents in the raw clay materials, RHA and the fired ceramic bricks with different RHA compositions and firing temperature is analyzed by XRD analysis. The XRD analysis allowed qualitatively weighting conversion, and the Rietveld refinement

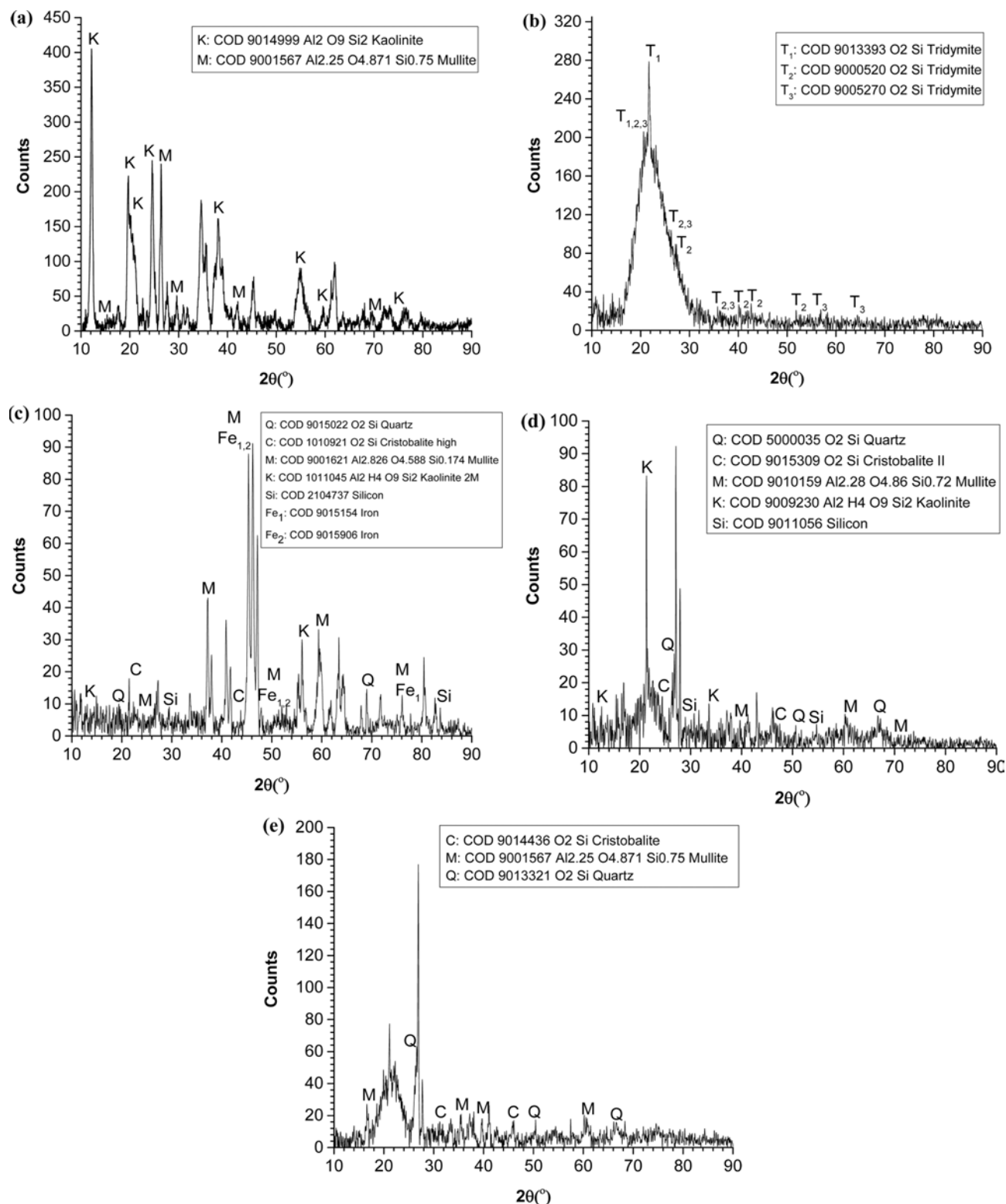


Fig. 7. XRD diffractogram of (a) China clay, (b) RHA, (c) R40 at 900 °C, (d) R40 at 950 °C and (e) R40 at 1,000 °C.

permitted to assess the conversion quantitatively [34]. The diffractograms observed from XRD analysis for selected RHA-based ceramic bricks are shown in Fig. 7.

Fig. 7(a) represent the diffractogram for the raw clay material used in this work. The extracted data from the diffractogram indicates that the crystallinity of the China clay is 64.7%. From the XRD analysis, it was observed that kaolinite (COD: 9014999) is the major mineral found in China clay while mullite (COD: 9001567) is the minor mineral. The natural crystal phase of China clay is quartz since it has a high amount of silica and alumina content. This quartz will transform into other crystal phases depending on the temperature it is being treated.

The diffractogram of RHA is depicted in Fig. 7(b). It is noticeable that an XRD single-phase amorphous of SiO_2 in RHA showed a diffused XRD peak with a maximum at about $2\theta = 21.8^\circ$ [4]. A similar observation is reported where XRD diffractogram revealed that RHA is mainly constituted by amorphous silica [35] with minor crystalline mineral of tridymite (COD: 9013390). Hence, this obtained data and literature-based evidence supported that the received RHA from the supplier is amorphous silica. In fact, silica in RHA is amorphous form when fired at low temperature in between 700°C to 800°C [36].

Then, crystallization of amorphous silica can occur at a higher temperature. Chandrasekhar et al. [4] reported that higher temperature caused the changes of amorphous of silica into crystalline polymorphs such as α -cristobalite, α -quartz and α -tridymite. There is also report that stated the possibility of phase coincides giving a single peak [5] due to the melting of the surface of ash silica particles followed by the formation of bonding of particle together [37, 38].

The difference between the amorphous and crystalline phase is that the amorphous has a broad peak and a wide angle of 2θ , while the crystalline phase has a pattern and a sharp peak [39]. This phase is clearly shown in Fig. 7(c-e) as compared to the amorphous phase in RHA, as shown in Fig. 7(b) previously. In addition, different XRD patterns as illustrated in Fig. 7(c-e) can be observed due to the effect of firing temperature on phase in the ceramic bricks. This indicated that the presence of new phases occurred at a high firing temperature.

For instance, at low temperature (900°C), the significant presence of quartz and mullite can be observed in Fig. 7(c). Then, the phase changed where the presence of cristobalite phase can be seen in Fig. 7(d). Different phases are present in the ceramic but with the different arrangement in their crystal structure. At higher temperature (950°C and $1,000^\circ\text{C}$), the intensity peak of quartz is reduced, mullite peak is constant but increase for cristobalite peaks. Thus, this observation can be asserted that different firing temperature is able to influence the grain growth and also the crystallinity

in the RHA-based ceramic bricks. Consequently, the physical properties (linear shrinkage, volumetric shrinkage and porosity) as reported earlier decreased with RHA content and firing temperature.

Conclusion

This preliminary conducted experiment regarding the effect of rice husk ash (RHA) and firing temperature in ceramic, particularly brick manufacturing properties is reported. The following conclusion can be drawn based on the obtained results:

a) The physical properties of the RHA-based ceramic bricks such as linear shrinkage, volumetric shrinkage and water absorption are decreased with the increment content of RHA and firing temperature.

b) The decrement in physical properties can be related to the presence of amorphous silica which causes unstable pore formation and boost for grains rearrangement which indicates that RHA is responsible partially for densification in ceramic and thus reduced the porosity.

c) However, the bulk density showed lower at higher RHA content and firing temperature, which can be related to the combustible of RHA at a higher temperature.

d) This observation is supported by XRF and XRD data which provided the composition and mineralogical properties of samples. Both of analysis found the presence of silica as mentioned previously and XRD data proved for the phases changes that occurred at the different firing temperature.

e) The sample with 20 wt.% of RHA and fired at 950°C showed potential as ceramic bricks due to the optimize differences in linear shrinkage, volumetric shrinkage, water absorption and bulk density among differing RHA contents at the same firing temperature.

f) These results suggest that the development of RHA-based ceramic bricks is a promising recycling method for low-cost and light-weight bricks production. Further analysis of using RHA in ceramic bricks, especially in thermal analysis need to be properly evaluated.

Acknowledgement

The authors would like to thank Faculty of Bioengineering and Technology, Universiti Malaysia Kelantan (UMK) for providing the research facilities to complete this project.

References

1. Selected Agricultural Indicators, Malaysia, 2019.
2. V.T.A. Van, C. Rößler, D.D. Bui, and H.M. Ludwig, Cem. Concr. Compos. 53 (2014) 270-278.
3. S.S. Hossain, L. Mathur, and P.K. Roy, J. Asian Ceram. Soc. 6[4] (2018) 299-313.

4. S. Chandrasekhar, K.G. Satyanarayana, P.N. Pramada, P. Raghavan, and T.N. Gupta, *J. Mater. Sci.* 38[15] (2003) 3159-3168.
5. S. Sultana, M. Rahman, Z. Yeasmin, S. Ahmed, and F.K. Rony, *J. Ceram. Process. Res.* 21[3] (2020) 285-295.
6. S.S. Hossain, L. Mathur, M.R. Majhi, and P.K. Roy, *J. Mater. Cycles Waste Manag.* 21[2] (2019) 281-292.
7. F.Z. Sobrosa, N.P. Stochero, E. Marangon, and M.D. Tier, *Ceram. Int.* 43[9] (2017) 7142-7146.
8. A. Samaddar, M. Mohibbe Azam, K. Singaravadeivel, N. Venkatachalapathy, B.B. Swain, and P. Mishra, in "TheFutur. Rice Strateg for India" (Elsevier Inc., 2017) p.301-334.
9. D. Eliche-Quesada, M.A. Felipe-Sesé, J.A. López-Pérez, and A. Infantes-Molina, *Ceram. Int.* 43[1] (2017) 463-475.
10. Y. Zou, and T. Yang, in "Rice Bran and Rice Bran Oil" (Elsevier Inc., 2019) p. 207-246.
11. E. Aprianti, P. Shafigh, S. Bahri, and J.N. Farahani, *Constr. Build. Mater.* 74 (2015) 176-187.
12. C.-L. Hwang, and T.-P. Huynh, *Constr. Build. Mater.* 93 (2015) 335-341.
13. J.O. Madu, F.V. Adams, B.O. Agboola, B.D. Ikotun, I.V. Joseph, *Mat. Proc. Today.* 38(2021) 599-604.
14. H.-S. Shin, and S.-T. Kang, *Water Res.* 37[1] (2003) 121-127.
15. S.K. Antiohos, V.G. Papadakis, and S. Tsimas, *Cem. Concr. Res.* 61-62 (2014) 20-27.
16. K.Y. Foo, B.H. Hameed, *Adv. In Col. And. Inter. Scie.* 152 (2009) 39-47
17. C.A.M. Moraes, I.J. Fernandes, D. Calheiro, A.G. Kieling, F.A. Brehm, M.R. Rigon, J.A.B. Filho, I.A.H. Schneider, E. Osorio, *Waste Manage. & Res.* 32 (2014) 1034-1048
18. P.T. Teo, A.S. Anasyida, C.M. Kho, M.S. Nurulakmal, *J. Clean. Product.* 241 (2019) 118144
19. L. Barbieri, F. Andreola, I. Lancellotti, and R. Taurino, *Waste Manag.* 33[11] (2013) 2307-2315.
20. Department of Statistics Malaysia, Special Release 2 (For Building and Structural Works), November 2020.
21. F. Andreola, I. Lancellotti, T. Manfredini, F. Bondioli, and L. Barbieri, *Waste and Biomass Valorization* 9[12] (2018) 2529-2539.
22. A. Ketov, V. Korotaev, L. Rudakova, I. Vaisman, L. Barbieri, and I. Lancellotti, *Int. J. Appl. Ceram. Technol.* 18[2](2020) 394-404.
23. I.J. Fernandes, F.A.L. Sánchez, J.R. Jurado, A.G. Kieling, T.L.A.C. Rocha, C.A.M. Moraes, and V.C. Sousa, *Adv. Powder Technol.* 28[4] (2017) 1228-1236.
24. J. Sutas, A. Mana, and L. Pitak, *Procedia Eng.* 32 (2012) 1061-1067.
25. M.P. Babisk, L.F. Amaral, L.D.S. Ribeiro, C.M.F. Vieira, U.S. Do Prado, M.C.B. Gadioli, M.S. Oliveira, F.S. Da Luz, S.N. Monteiro, and F.D.C. Garcia Filho, *J. Mater. Res. Technol.* 9[2] (2020) 2186-2195.
26. C. Bories, L. Aouba, E. Vedrenne, and G. Vilarem, *Constr. Build. Mater.* 91 (2015) 158-163.
27. S. Lawanwadeekul, T. Otsuru, R. Tomiku, and H. Nishiguchi, *Constr. Build. Mater.* 255 (2020) 119376.
28. V. Loryuenyong, T. Panyachai, K. Kaewsimork, and C. Siritai, *Waste Manag.* 29[10] (2009) 2717-2721.
29. I.W.M. Brown, K.J.D. MacKenzie, M.E. Bowden, and R.H. Meinheld, *J. Am. Ceram. Soc.* 68[6] (1985) 298-301.
30. A. Balasubramanian, *Use of Clay in Pottery*, 2017.
31. M. Du, J.-Q. Bi, W.-L. Wang, X.-L. Sun, and N.-N. Long, *Mater. Sci. Eng. A* 543 (2012) 271-276.
32. S. Janbuala, and T. Wasanapiampong, *Key Eng. Mater.* 659 (2015) 74-79.
33. S. Rajpoot, R. Malik, and Y.W. Kim, *Ceram. Int.* 45[17] (2019) 21270-21277.
34. M.F. Serra, M.S. Conconi, M.R. Gauna, G. Suárez, E.F. Aglietti, and N.M. Rendtorff, *J. Asian Ceram. Soc.* 4[1] (2016) 61-67.
35. E.M.M. Ewais, R.M. Elsaadany, A.A. Ahmed, N.H. Shalaby, and B.E.H. Al-Anadoul, *Refract. Ind. Ceram.* 58[2] (2017) 136-144.
36. S.S. Cole, *J. Am. Ceram. Soc.* 18[1-12] (1935) 149-154.
37. Y. Nakata, M. Suzuki, T. Okutani, M. Kuchi, and T. Akyama, *J. Ceram. Soc. Japan* 97[1128] (1989) 842-849.
38. J.J.F. Saceda, R.L. De Leon, K. Rintramee, S. Prayoonpokarach, and J. Wittayakun, *Quim. Nova* 34[8] (2011) 1394-1397.
39. I. Johari, S. Said, R.P. Jaya, B.H.A. Bakar, and Z.A. Ahmad, in *Proceedings of the International Conference on Environment Science and Engineering*, April 2011, (IACSIT Press, Singapore, 2011) pp. 171-174.